CARBON 48 (2010) 2873–2881

available at www.sciencedirect.com

ScienceDirect

journal homepage: www.elsevier.com/locate/carbon

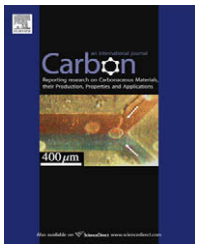

Raman intensity measurements of single-walled carbon nanotube suspensions as a quantitative technique to assess purity

Veronica M. Irurzun, M. Pilar Ruiz, Daniel E. Resasco *

School of Chemical, Biological and Materials Engineering, Carbon Nanotube Technology Center (CANTEC), University of Oklahoma, 100 East Boyd Street, Norman, OK 73019, United States

ARTICLE INFO

Article history:
Received 14 December 2009
Accepted 12 April 2010
Available online 14 April 2010

ABSTRACT

A method to assess the purity of single-walled carbon nanotube (SWCNT) bulk samples based on Raman spectroscopy is reported. The new method has higher reproducibility and quantitative precision than those previously used. It consists of measuring the G-band intensity of liquid suspensions of SWCNT samples as a function of solid concentration. A simple equation is proposed in which one of the two adjustable parameters is the SWCNT purity. The method has been applied to a series of samples of similar characteristics, but varying quality. The results are compared to those obtained on the same series of samples using standard analytical techniques, including electron microscopy, thermogravimetric analysis and optical absorption.

1. Introduction

Assessment of purity and quantification of single-walled carbon nanotubes (SWCNT) in bulk samples is crucial in the production of nanotubes for commercial or scientific applications. Knowing with some degree of precision the SWCNT concentration in a given sample gives the application researchers the possibility of comparing the effects of adding varying amounts of SWCNT to the composite material [1–3] or devices [4–9] that they are developing. A good quantification of SWCNT concentration in a sample can also allow researchers to do proper comparison of SWCNT from different sources, or with varying structural characteristics.

Raman spectroscopy has been widely used to assess SWCNT quality. For example, the full width at half maximum (FWHM) of the Raman D-band (~1350 cm^{-1}) has been used by several researchers [10–13]. The FWHM D-band of the non-SWCNT carbonaceous species is generally much broader than that of the SWCNT. Likewise, the absolute intensity of the G and D-bands (~1590 cm^{-1}, ~1350 cm^{-1}) [11,14,15] and, the G/D and D/G′ ratios [11,16–20] have been used to measure the quality of SWCNT. The G/D ratio is generally considered as a quality parameter because the G-band, being a first-order Raman scattering process is not affected by defects. By contrast, the D-band is a second-order Raman scattering process that is enhanced by the presence of defects.

The use of the G/D ratio as a quantification method for the density of defects has generated some controversy. For instance, Antunes et al. [12] have shown that the intensity of the D-band is affected by curvature effects. They have proposed that the product of the D/G intensity ratio and the FWHM of the D-band is a better indicator of CNT quality. A method that may simplify the problem was proposed by Nishide et al. [14]. This work has pointed out that the Raman intensity of SWCNT is highly enhanced by resonance effects, but these effects are much weaker in amorphous carbon. Therefore, these authors concluded that the absolute intensity of the G-band may be a more suitable quality parameter than the D/G ratio. Different authors have measured the shift between the second and the first order transitions [21], and

* *Corresponding author:* Fax: +1 405 325 5813.
E-mail address: resasco@ou.edu (D.E. Resasco).
0008-6223/$ - see front matter
doi:10.1016/j.carbon.2010.04.019

used these values to quantify the purity of SWCNT in a sample. Another approach for assessing SWCNT quality is a technique proposed by Liu et al. [22] in which Raman scattering is combined with photoluminescence.

In general, these quality assessment methods have been conducted on solid samples, which have the serious drawback of composition heterogeneity and variations in texture. If not properly weighted, these variations may greatly affect the results and yield wrong estimates of the purity. In this contribution, we propose a modified Raman analysis method that results in a reliable quantitative assessment of SWCNT purity.

2. Experimental

2.1. Materials

The CoMoCAT process, developed by our group in 1998 [23] and further improved during subsequent years [24–27], has been optimized for large-scale production and commercialization by SouthWest Nanotechnologies (SWeNT). During this process, the influence of different operating parameters has been investigated. Among them, temperature of calcination, reduction, and growth, as well as space velocity (gas flow rate/catalyst volume ratio), reaction time, reactor design, operation, etc., have been found to have a strong influence on nanotube yield, nanotube type, and purity. From these optimization studies a range of SWCNT samples with varying degrees of quality and purity have been obtained. In the present study, a series of samples of varying quality and purity has been prepared to evaluate the quality assessment method.

The growth of SWCNT for all samples was carried out on the same type of powder catalyst composed of Co–Mo particles supported on high-surface area silica, with a total metal loading of 2 wt.% and a Co–Mo molar ratio of 1/2. Before starting the growth reaction, the catalyst was reduced in H_2 flow at 500 °C for 30 min. Then, H_2 was replaced by He, while increasing the temperature to 700 °C. At this temperature, the catalyst was placed in contact with carbon monoxide (CO) for 30 min. After the growth period, the system was cooled down under He flow. To separate the SWCNT product from the catalyst, the as-produced material was treated in 30% HF solution, which completely dissolved the silica support. To eliminate the metal species (Co and Mo) the sample was further treated in an HCl solution. After these treatments the samples contained about 8 wt.% Co and Mo, with no traces of Si or any other element.

Two external samples of known SWCNT content were employed as reference points in the purity scale. A carbon black sample was used as the standard for zero SWCNT content. The sample to be considered as of maximum purity (100%) was provided by the National Institute of Standards and Technology (NIST), where it is identified as VAMAS TWA 34. The sample itself is a length-sorted SWCNT dispersion in an aqueous 1% (mass/vol) sodium deoxycholate solution. The estimated concentration of nanotubes in the original sample was about 50 mg/L. This sample was taken from the liquid that will become a NIST reference material for dispersed, length sorted, carbon nanotubes (RM 8281 "Long" fraction, estimated average length ~0.75 μm).

The synthesized samples were purified again by using a method proposed by Miyata et al. [28], which includes sonication, suspension in sodium cholate, 1-h ultra-centrifugation at 207,000*g*, and collection of the supernatant fractions. The intensity of the Raman G-band was measured for all the ultra-purified samples and correlated to the relative concentration of SWCNT in the sample. For comparison, seven as-produced solid SWCNT samples, still associated with the silica-supported catalyst, were analyzed by Raman scattering.

Specifically, aqueous suspensions of the different SWCNT samples were prepared by placing 5 mg of purified SWCNT in 7 ml of 2 wt.% solution of sodium cholate (SC) in deionized water (DI) and ultra-sonicating with a Horn Sonic Dismembrator, Model 500, Fisher Scientific for 1 h at 7 mW of power. To compare these sonicated suspensions at the same total solid concentration the following method was followed. First, the optical absorption of the suspension was measured at a wavelength of 770 nm. Then, the concentration of all the suspensions, including the reference from NIST, was adjusted to obtain the same absorptivity for each one by diluting with deionized water. A value of relative concentration equal to 1.0 was arbitrarily assigned to each suspension with an absorption coefficient of 0.85. To study the variation of Raman intensity with concentration, various dilutions were prepared for each sample.

2.2. Characterization methods

Several methods were combined to assess the SWCNT quality of the samples in the series. Raman spectroscopy of the suspensions was conducted in a Jovin Yvon-Horiba Lab spectrometer, equipped with a CCD detector and with a laser excitation of 633 nm (He–Ne laser). Eight spectra were taken for each sample, varying the concentration by diluting with deionized water. In addition to the measurements on liquid suspensions, Raman spectra were obtained on solid samples. In this case, the collection time for each measurement was 10 s; to assure that the measurements provided an average that was representative of a given sample, 50 measurements on different spots were taken on each sample. The G/D ratio and the FWHM of the D-band were used as quality indicators. The same SWCNT suspensions used in Raman characterization were characterized by Optical Absorption (OA) in an UV–Vis (UV-2101PC, Shimadzu spectrophotometer). Images of the purified samples were obtained by Transmission (JEOL 2000-FX STEM), and Scanning Electron Microscopy (JEOL JSM-880 SEM). The samples analyzed by TEM were prepared by suspending the SWCNT by mild sonication in isopropanol and depositing a drop over the TEM grid. The samples analyzed by SEM were deposited onto copper strips and coated with gold and palladium. Thermo Gravimetric Analysis (TGA) of purified samples was conducted in a TGAQ500 (TA instruments Inc.) under flow of air at 200 °C for 15 min and heated to 750 °C at a rate of 5 °C/min.

The as-produced solid SWCNT samples from the synthesis reactor were characterized using Raman spectroscopy. The collection time in each spot and number of spots probed for the as-produced solid sample were the same as those for the purified samples (10 s, 50 spots). As discussed below, these measurements allowed us to evaluate the level of

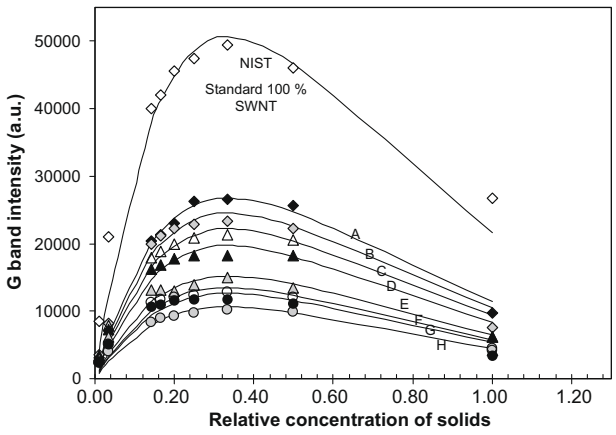

Fig. 1 – G-band intensity of SWCNT suspensions of varying concentrations relative to those showing the same absorption intensity.

heterogeneity in each sample and to obtain a representative average of the quality parameters.

3. Results and discussion

3.1. *Raman scattering of purified SWCNT samples*

3.1.1. *SWCNT suspensions*

Nishide et al. [14] have proposed to use the G-band intensity of nanotube suspensions as an indication of the purity of a SWCNT sample. In this study we have found that this intensity is not only a function of the purity of the SWCNT sample but also of the overall solid concentration of the suspension. As shown in Fig. 1 the G-band intensity (I_G^{LIQ}) exhibits a characteristic profile as a function of relative concentration. As the concentration decreases from the initial value (1.0), the scattering intensity increases, reaching a maximum at about the same concentration for all the samples and then it decreases with further dilution. This "thickness effect" is typically observed when the light scattering initially increases with increasing concentration, but it is attenuated at higher concentrations by absorption. In this particular case, while the Raman scattered radiation is entirely due the SWCNT scatterers present in the suspension, the absorption is caused by all the suspended species (attenuators). The fraction of incoming radiation scattered is proportional to the concentration of SWCNT since the scattering cross section of SWCNT is much larger than any other suspended species. But, at the same time, the absorption of both incoming and outgoing radiation is due to the relative concentration (C) of all the suspended species. Therefore, we can express the variation of the scattered radiation as a function of carbon concentration with the following equation:

$$\frac{I_S}{I_0} = PCe^{-SC} \quad (1)$$

where I_S and I_0 represent the effective scattered radiation and incoming radiation intensities, respectively. P is the fraction of SWCNT in each sample and S is a proportionality constant that is common for all samples. This equation has been used to fit the experimental data of intensity of the scattered G-band as a function of concentration of solids in the suspension. Using only P and S as adjustable parameters, the fitting for all the samples is very good and provides values of the fraction of SWCNT (P) for each sample (see solid lines in Fig. 1).

By fixing the P factor obtained for the NIST reference sample as corresponding to 100% SWCNT we can obtain direct estimates of the fraction of SWCNT in each sample. The corresponding P factors for all the samples in the series are shown in Table 1. The samples are identified as A-to-H in order of decreasing quality.

3.1.2. *Solid samples*

One of the most important aspects that need to be addressed when assessing the quality of SWCNT solid samples is heterogeneity. However, it has been common practice to assess SWCNT sample quality averaging G/D ratios of only a few (e.g., one to three) Raman measurements [24,29–32]. Table 1 shows the average G/D Raman intensity ratios obtained on the samples in the series by using only three spots (G/D 3). As illustrated in Fig. 2, a poor correlation is obtained between the P factor obtained with the suspensions and the G/D 3 ratios obtained from averaging only three spots on the solid samples.

A much more representative average can be obtained by increasing the number of measurements. For instance, Fig. 3 shows the rather high variability in the G/D ratios obtained

Table 1 – Quality values obtained by using different characterization techniques. P (%) values obtained from Raman of the liquid suspensions. SWCNT area/total area obtained from TGA analysis. Resonance factor obtained from OA analysis. G/D (ap), G/D 3, G/D 50 and 1/FWHM D-band obtained from Raman of the solid samples.

Sample	Raman suspensions	TGA	UV–Vis	Raman solids			
	P (%)	SWCNT area/total area	Resonance factor (×100)	G/D (ap)	G/D 3	G/D 50	1/FWHM D-band (×100)
NIST ref	100.00	–	–	–	–	–	–
A	52.90	1.00	7.73	29.00	–	–	–
B	48.30	1.00	7.32	23.00	11.20	11.68	5.00
C	43.80	0.77	7.03	22.90	11.00	9.06	3.60
D	38.90	0.85	6.65	18.80	13.10	8.60	4.00
E	30.00	0.65	4.43	18.50	6.00	7.21	3.40
F	26.70	0.29	2.77	20.70	1.40	4.93	2.70
G	24.80	0.42	3.91	13.70	7.90	6.32	3.20
H	20.90	0.49	2.76	4.50	7.60	7.98	3.30

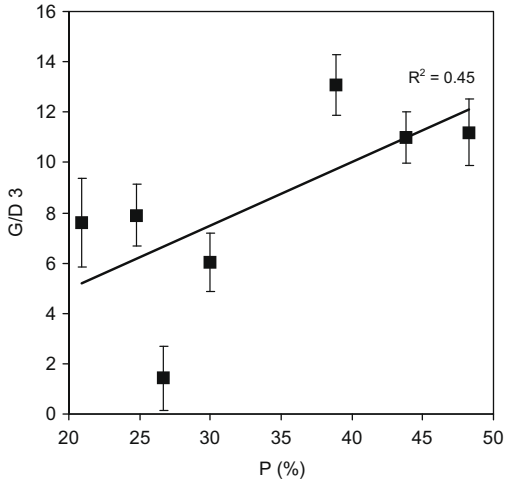

Fig. 2 – Comparison of the P (%) quality parameter values with the G/D ratios of the solid samples by averaging three spots (G/D 3).

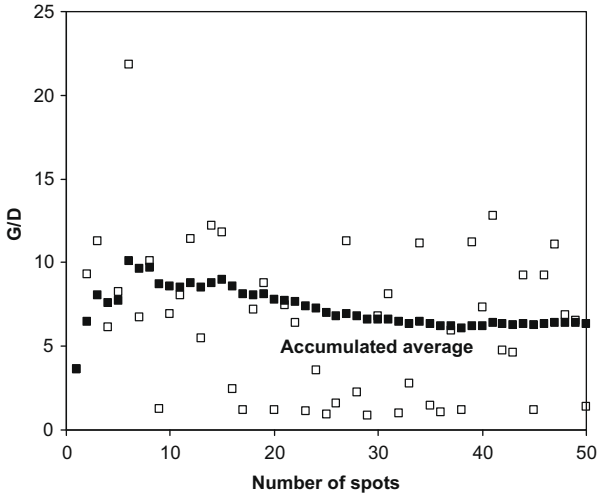

Fig. 3 – G/D accumulated average and the singular G/D ratios of solid samples for 50 different spots (Sample G).

on 50 different spots on a given sample together with the accumulated average, which as expected shows gradually lower variability as the number of measurements increase. Similar analysis was done for each solid sample in the series and the results of accumulated averages are compared in Fig. 4(a). It can be seen that depending on the variability of the specific sample one may need 30 or more spots to obtain a reliable average. We have used a common statistical method [33] to establish margins of error (E) in a number of measurements (n) with a given level of confidence, based on the following expression $E = z\ (\sigma/\sqrt{n})$, in which σ is the standard deviation and z is calculated from the desired level of confidence. For example, for a level of confidence of 95% and assuming a standard normal distribution of the measurements, z becomes 1.96 [33]. Then for $n = 50$ measurements, the margins of error can be readily obtained for each sample (Margins of error for G/D 50 values – B: 1.33, C: 1.02, D: 1.2, E: 1.28, F: 1.76, G: 1.23, H: 1.15).

Fig. 4(b) shows the accumulated average of the 1/FWHM of the D-band as a function of the number of measurements. The general trend shows that as the quality of the sample increases, the D-band width decreases and therefore 1/FWHM D-band increases. Since the D-band is a convolution of different bands related to different defective carbon species, the more species there are in the sample, the broader will be the width. Table 1 shows the average for each sample. The margin of error for $n = 50$ measurements were obtained for each sample (Margins of error for 1/FWHM D-band ($\times 10^3$) – B: 0.34, C: 0.35, D: 0.37, E: 0.34, F: 0.39, G: 0.41, H: 0.51). While the overall trend is that the G/D ratio increases and the width of the D-band decreases from the lowest-quality sample to the highest-quality sample, there are a few samples of intermediate quality in which it is hard to make a decision about which one has a higher SWCNT content.

Taking P of the suspensions as a measure of the fraction of SWCNT in the sample, we have plotted in Fig. 5 the variation of the G/D 50 average ratio and the 1/FWHM of the D-band in the purified solid samples with P in the suspensions to compare the goodness of each method. In this case, the correlation of P and G/D 50 is clearly much better than when few spots were used. The correlation factors for G/D 50 and 1/FWHM of the D-band with P are 0.89 and 0.73, respectively, which are significantly higher than those obtained with three spots (0.45 and 0.41, respectively).

3.2. *Scanning and transmission electron microscopy (SEM–TEM)*

Electron microscopy provides a visual assessment of the overall quality of the sample, but assessment of the fraction of SWCNT by microscopy methods is at best semi-quantitative and in most cases, the imaged fraction of the sample may not be fully representative of the entire sample [34]. With these limitations in mind, a qualitative comparison of the various samples in the series has been attempted. Fig. 6 shows the SEM images of all the samples in the series. To compare with the Raman results, the images were ordered by observation of purity and quality, starting with the one with the highest fraction of SWCNT present. The qualitative order obtained by SEM coincides very well with the quantitative P factor obtained from the Raman analysis of the suspensions. The samples with low P factor showed few SWCNT and larger quantities of non-SWCNT carbonaceous species and residual catalyst. Samples with intermediate values of P showed comparable amounts of SWCNT and impurities. Samples with the highest P factors exhibited only SWCNT in the SEM image.

The TEM images for samples B and F compared in Fig. 7(a) and (b) clearly show the differences between high-quality and low-quality samples. The high-quality sample B is mainly composed of SWCNT with small catalyst particles remaining. On the other hand, the low-quality sample F exhibits other carbon structures like fibers and MWCNT as well as relatively large catalyst particles.

3.3. *Thermo gravimetric analysis (TGA)*

In TGA the weight change caused by oxidation of carbonaceous species is monitored in a microbalance [35]. This tech-

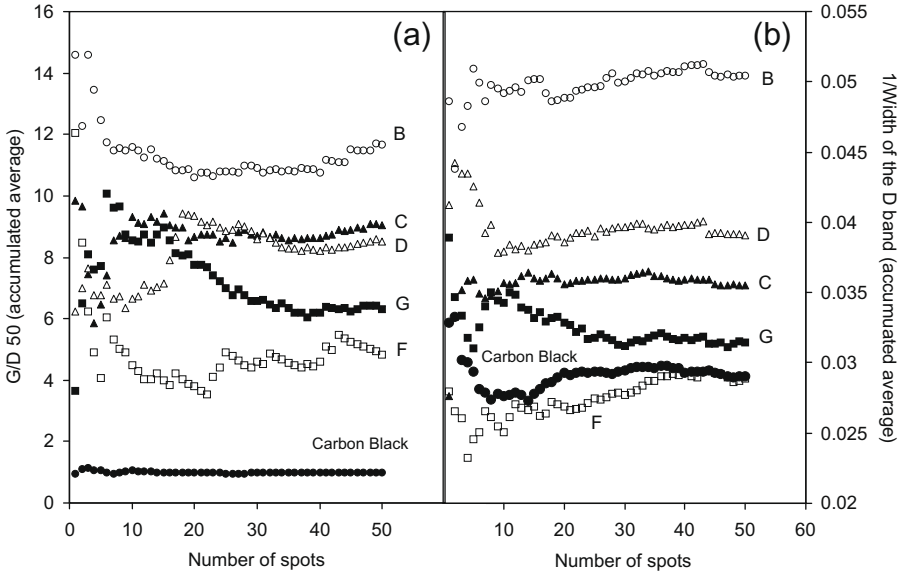

Fig. 4 – Accumulated average values (50 spots) of solid samples with different purities. (a) G/D ratios; (b) 1/FWHM of the D-band.

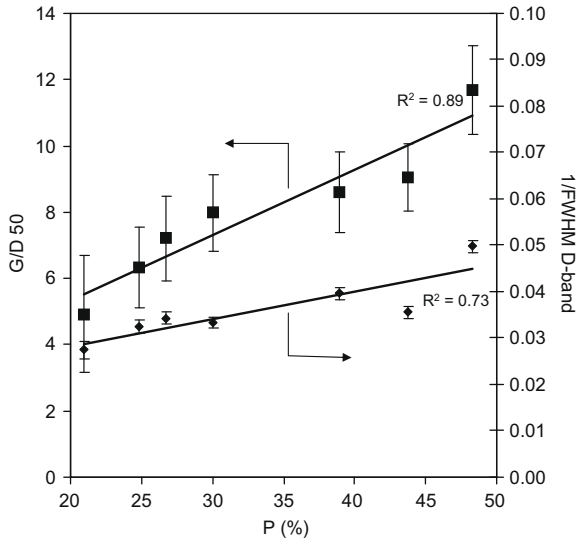

Fig. 5 – G/D 50 ratios-1/FWHM of the D-band vs. the *P* (%) quality parameter values.

nique is typically used to obtain semi-quantitative estimates of the fraction of SWCNT in a sample but, as we discuss below, it is not a precise quantitative technique. Fig. 8(a) shows the TGA profiles for two samples of the series, one with a high fraction of SWCNT (B, *P* = 48.3%) and one with low fraction (F, *P* = 26.7%). While the profile for the good sample B exhibits only one peak, the lower quality sample F shows two. The peak appearing at the lower temperature is typically ascribed to the oxidation of SWCNT while the one at higher temperatures is related to other carbonaceous species, e.g. graphitic nano-fibers [35]. The TGA results, reported as the ratio of the area of low-temperature peak over the total area, are included in Table 1. At the same time, Fig. 8(b) compares the TGA data with the SWCNT fractions as estimated from the *P* factors. Again, while the general trend is in agreement, the correlation factor is relatively low, 0.68.

It must be pointed out that the TGA method has some significant limitations that may affect the results. First, it must be noted that carbon oxidation reaction occurring in TGA can be significantly altered by the presence of metal impurities that can act as oxidation catalysts [36,37]. Second, the state of aggregation of the samples may significantly affect the rate of mass and heat transfer during the oxidation reaction and as a result can cause peak shifts in TGA. These two features are sometimes ignored but they may vary significantly from sample to sample causing significant differences in the estimated SWCNT purities.

To illustrate these limitations of the technique, a clear example of the effects of aggregation on the TGA profile is shown in Fig. 9. In this case, both profiles correspond to exactly the same purified SWCNT sample, but one of the aliquots was oven-dried after purification while the other was freeze-dried. It is known that the former drying method results in higher extent of agglomeration than the latter. Clearly, the more highly agglomerated sample exhibited an enhanced fraction of carbon oxidizing at the high-temperature region compared to the freeze-dried sample, with a more open structure. This dramatic difference indicates that unless the level of impurities and state of agglomeration are kept constant, TGA can lead to erroneous measurements of SWCNT purity.

3.4. *Optical absorption (OA)*

Optical absorption is a powerful technique that can be effectively employed to measure the type and quality of SWCNT in a sample [38–41]. The absorption spectrum of SWCNT exhibits the characteristic bands of the 1-dimensional van Hove singularities. Semiconducting SWCNT give rise to transitions between mirror singularities in the electronic density of states

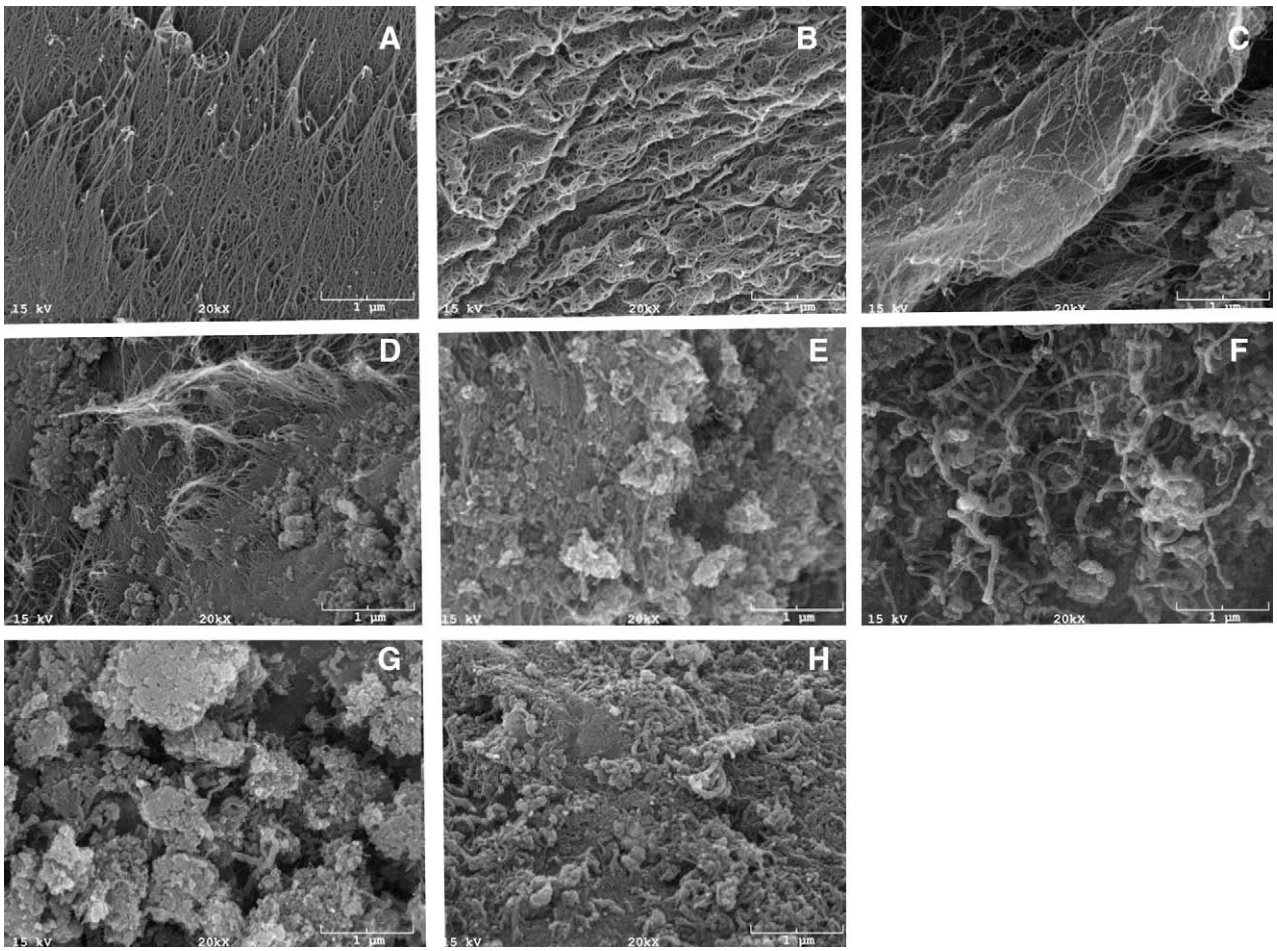

Fig. 6 – SEM images of the purified solid samples series.

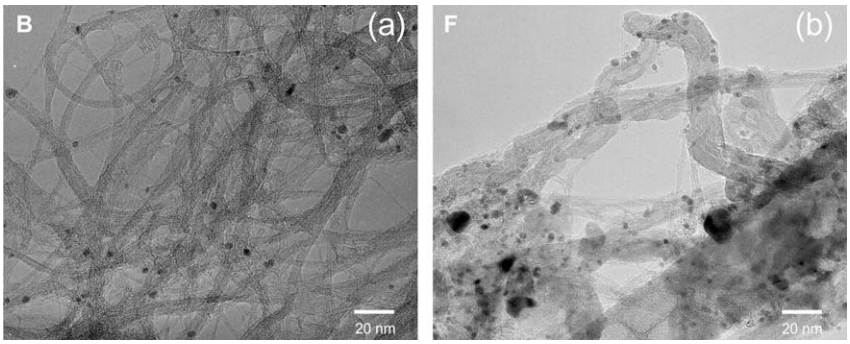

Fig. 7 – TEM images. (a) High quality (sample B); (b) Low quality (sample F).

termed S_{11}, S_{22}, etc. Integrating intensity of these bands and the spectral background provides a valuable parameter that can be used to estimate the purity of the sample. Itkis et al. [42] have developed a method that relates the area of the S_{22} transition and the total area under the spectra to the purity of the sample. A similar method was developed to evaluate the effectiveness of surfactants and dispersion methods on the same CoMoCAT sample [43]. Some of the limitations of these methods are the uncertainty associated with the position of the spectral background and the variation of the absorption intensity with the state of dispersion [41]. More recently, Landi et al. [39] developed a modified version of this method that enhances its accuracy, as verified on a series of samples constructed with specific mass fractions of purified SWCNT and other carbonaceous species. This modified method is based on a non-linear plasmon model that includes the overlap of the transitions and peak broadening. To ensure accuracy of the fitting, it is important that the spectrum covers high enough energies as to reach the maximum plasmon intensity, occurring at about 4.5–5 eV.

Fig. 10(a) shows the UV–Vis spectra of samples C and H, which according to the Raman *P* factors have fractions of

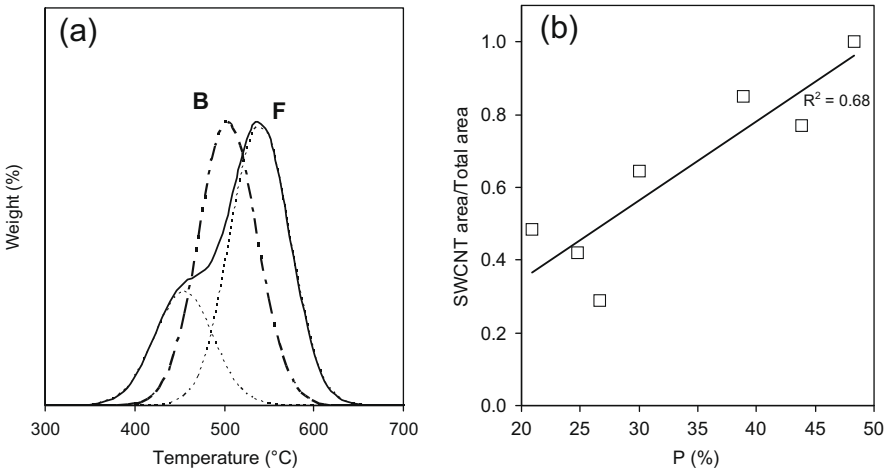

Fig. 8 – (a) TGA profiles of the purified solid samples B and F; (b) Comparison of the P (%) quality parameter values with the quality values obtained from TGA.

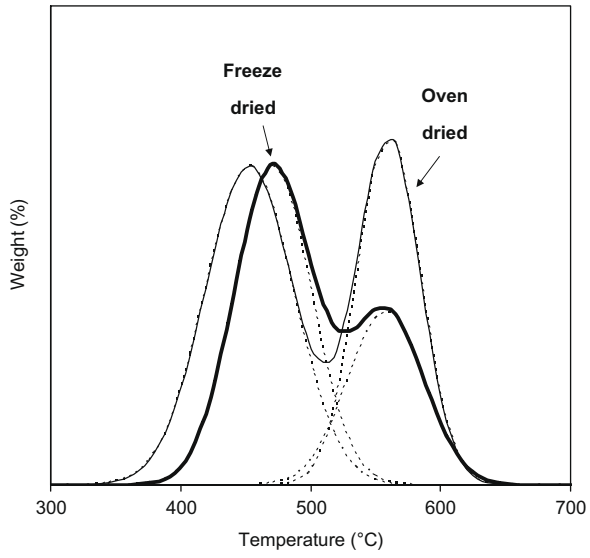

Fig. 9 – TGA profiles for the same sample with different state of aggregation.

SWCNT of about 43.8% and 20.9%, respectively. As mentioned above, the intensity of characteristic bands in the absorption spectrum intensity relative to the spectral background should correlate with the purity of the sample [42,43]. In good correlation with the prediction from the intensity of the Raman G-band of the suspensions, it is seen that the ratio of areas under the resonance bands to the background drop by about a factor of two from sample C to sample H. The resonance factors calculated according to Tan et al. [43] are summarized in Table 1. To compare the correlation of these values with those from the Raman method, Fig. 10(b) shows the variation of the resonance factor with P for all the samples in the series. The correspondence between the two methods is very good, i.e., the correlation factor is 0.92.

3.5. *As-produced SWCNT samples*

In most CVD methods used in the synthesis of SWCNT, the active metal catalysts are typically deposited on a high-surface area support in relatively low concentrations. As such, a large fraction of the as-produced material consists of the

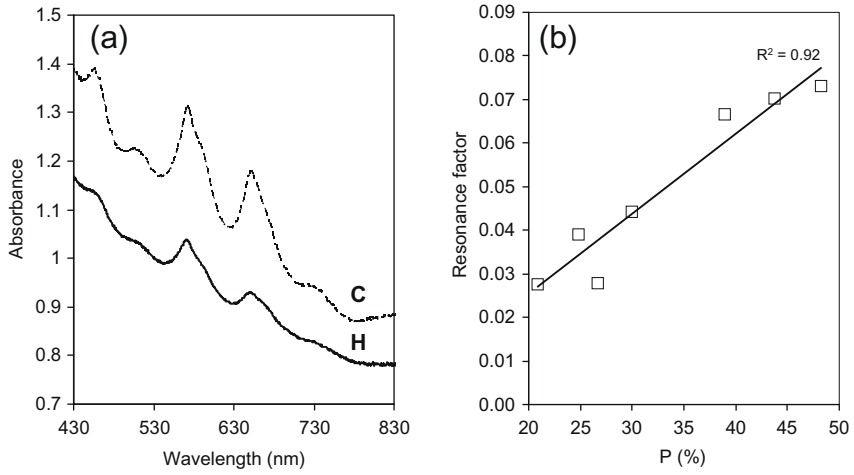

Fig. 10 – (a) UV–Vis spectra of suspensions prepared from purified solid samples C and H; (b) comparison of the P (%) quality parameter values with the resonance factors obtained from the OA analysis.

catalyst support, which needs to be separated from the SWCNT by chemical or mechanical means. In the particular case of the CoMoCAT method employed in this study, the as-produced material contained 5–7 wt.% C, 1–2 wt.% Co–Mo, and the rest SiO_2. The as-produced solid material was analyzed by Raman scattering and the G/D ratios obtained are compared to those obtained on the purified samples.

The G/D ratios obtained for the as-produced samples (G/D (ap)) are included in Table 1 together with those obtained for the purified samples. It can be seen that while the trend for the series is the same as that of the corresponding purified samples, the absolute G/D ratios for the as-produced samples were significantly larger than those for the purified samples. That is, while the G/D ratios are still high in the purified samples, it is evident that the purification process enhances the intensity of the D-band, either by creating defects or by generating functionalized groups on the SWCNT walls. Similar reductions in G/D ratios after purification have been reported and ascribed to partial doping caused by the acid treatment, which may reduce the resonant Raman response [42,44].

4. Conclusions

The assessment of quality and purity of SWCNT bulk samples is complicated by the heterogeneity of solid samples. Most methods employed to date exhibit some limitations. The method most commonly used is Raman spectroscopy. However, to overcome the problem of sample heterogeneity and to obtain reliable and quantitative estimates of the percent of SWCNT in a sample one needs a large number of measurements. By contrast, the measurement of G/D ratio in liquid suspensions as a function of solid concentration provides a more practical and reliable method than those previously used. A simple equation with two adjustable parameters can be used to directly extract the percent of SWCNT in the sample.

Acknowledgements

The project was financially supported by the Department of Energy-Basic Energy Sciences (Grants DEFG03-02ER15345 and DE-FG02-06ER64239) and the Oklahoma State Regents for Higher Education. SEM and TEM characterization was conducted in the Samuel Roberts Noble Electron Microscopy Laboratory at the University of Oklahoma.

REFERENCES

[1] Ramasubramaniam R, Chen J, Liu H. Homogeneous carbon nanotubes/polymer composites for electrical applications. Appl Phys Lett 2003;83(14):2928–30.
[2] Shim BS, Tang Z, Morabito MP, Agarwal A, Hong H, Kotov NA. Integration of conductivity, transparency, and mechanical strength into highly homogeneous layer-by-layer composites of single-walled carbon nanotubes for optoelectronics. Chem Mater 2007;19:5467–74.
[3] Nepal D, Balasubramanian S, Simonian AL, Davis VA. Strong antimicrobial coatings: single-walled carbon nanotubes armored with biopolymers. Nano Lett 2008;8(7):1896–901.
[4] Li Z, Biris AS, Dervishi E, Saini V, Xu Y, Biris AR, et al. Influence of impurities on the X-ray photoelectron spectroscopy and Raman spectra of single-wall carbon nanotubes. J Chem Phys 2007;127(1546713):1–7.
[5] Kruusma J, Mould N, Jurkschat K, Crossley A, Banks CE. Single walled carbon nanotubes contain residual iron oxide impurities which can dominate their electrochemical activity. Electrochem Commun 2007;9:2330–3.
[6] Liu B, Ren W, Gao L, Li S, Pei S, Liu C, et al. Metal-catalyst-free growth of single-walled carbon nanotubes. J Am Chem Soc 2009;131(6):2082–3.
[7] Jones CP, Jurkschat K, Crossley A, Compton RG, Riehl BL, Banks CE. Use of high-purity metal-catalyst-free multiwalled carbon nanotubes to avoid potential experimental misinterpretations. Langmuir 2007;23(18):9501–4.
[8] Penza M, Tagliente MA, Aversa P, Re M, Cassano G. The effect of purification of single-walled carbon nanotubes bundles on the alcohol sensitivity of nanocomposite. Langmuir–Blodgett films for saw sensing applications. Nanotechnology 2007;18:185502–14.
[9] Johnston DE, Islam MF, Yodh AG, Johnson AT. Electronic devices based on purified carbon nanotubes grown by high-pressure decomposition of carbon monoxide. Nature Mater 2005;4:589–92.
[10] Dillon AC, Yudasaka M, Dresselhaus MS. Employing Raman spectroscopy to qualitatively evaluate the purity of carbon single-wall nanotube materials. J Nanosci Nanotechnol 2004;4(7):691–703.
[11] Lee S, Peng JW, Liu CH. Probing plasma-induced defect formation and oxidation in carbon nanotubes by Raman dispersion spectroscopy. Carbon 2009;47:3488–97.
[12] Antunes EF, Lobo AO, Corat EJ, Trava-Airoldi VJ. Influence of diameter in the Raman spectra of aligned multi-walled carbon nanotubes. Carbon 2007;45:913–21.
[13] Jorio A, Fantini C, Dantas MSS, Pimenta MA, Souza Filho AG, Samsonidze GEG, et al. Linewidth of the Raman features of individual single-wall carbon nanotubes. Phys Rev B 2002;66(115411):1–8.
[14] Nishide D, Kataura H, Suzuki S, Tsukagoshi K, Aoyagi Y, Achiba Y. High-yield production of single-wall carbon nanotubes in nitrogen gas. Chem Phys Lett 2003;372:45–50.
[15] Musumeci AW, Waclawik ER, Frost RL. A comparative study of single-walled carbon nanotube purification techniques using Raman spectroscopy. Spectroquim Acta A 2008;71:140–2.
[16] Simpson JR, Fagan JA, Becker ML, Hobbie EK, Hight Walker AR. The effect of dispersant on defects in length-separated single-wall carbon nanotubes measured by Raman spectroscopy. Carbon 2009;47:3238–41.
[17] Delhaes P, Couzi M, Trinquecoste M, Dentzer J, Hamidou H, Vix-Guterl C. A comparison between Raman spectroscopy and surface characterizations of multiwall carbon nanotubes. Carbon 2006;44(14):3005–13.
[18] Kobayashi Y, Takagi D, Ueno Y, Homma Y. Characterization of carbon nanotubes suspended between nanostructures using micro-Raman spectroscopy. Phys E 2004;24(1–2):26–31.
[19] Qian W, Liu T, Wei F, Yuan H. Quantitative Raman characterization of the mixed samples of the single and multi-wall carbon nanotubes. Carbon 2003;41:1851–4.
[20] Heise HM, Ruckuk R, Ojha AK, Srivastava A, Srivastava V, Asthana BP. Characterization of carbonaceous materials using Raman spectroscopy: a comparison of carbon nanotube filters, single- and multi-walled nanotubes, graphisited porous carbon and graphite. J Raman Spectrosc 2009;40(3):344–53.

[21] Thomsen C. Second-order Raman spectra of single and multiwalled carbon nanotubes. Phys Rev B 2000;61(7):4542–4.
[22] Liu T, Xiao Z, Wang B. The exfoliation of SWCNT bundles examined by simultaneous Raman scattering and photoluminescence spectroscopy. Carbon 2009;47:3529–37.
[23] Resasco DE, Kitiyanan B, Harwell JH, Alvarez W. Method of producing carbon nanotubes. US Patent No. 6333016, 2001.
[24] Lolli G, Zhang LA, Balzano L, Sakulchaicharoen N, Tan Y, Resasco DE. Tailoring (*n*, *m*) structure of single-walled carbon nanotubes by modifying reaction conditions and the nature of the support of CoMo catalysts. J Phys Chem B 2006;110(5):2108–15.
[25] Alvarez WE, Pompeo F, Herrera JE, Balzano L, Resasco DE. Characterization of single-walled carbon nanotubes (SWCNTs) produced by CO disproportionation on Co–Mo catalysts. Chem Mater 2002;14(4):1853–8.
[26] Resasco DE, Alvarez WE, Pompeo F, Balzano L, Herrera JE, Kitiyanan B, et al. A scalable process for production of single-walled carbon nanotubes (SWCNT) by catalytic disproportionation of CO on a solid catalyst. J Nanopart Res 2002;4(1–2):131–6.
[27] Resasco DE, Herrera JE, Balzano L. Decomposition of carbon-containing compounds on solid catalysts for single-walled nanotubes production. J Nanosci Nanotechnol 2004;4(4):398–407.
[28] Miyata Y, Yanagi K, Maniwa Y, Tanaka T, Kataura H. Diameter analysis of rebundled single-wall carbon nanotubes using X-ray diffraction: verification if chirality assignment based on optical spectra. J Phys Chem C 2008;112:15997–6001.
[29] Herrera JE, Resasco DE. In situ TPO/Raman to characterize single-walled carbon nanotubes. Chem Phys Lett 2003;376(3–4):302–9.
[30] Strong KL, Anderson DP, Lafdi K, Kuhn JN. Purification process for single-wall carbon nanotubes. Carbon 2003;41:1477–88.
[31] Li Q, Yan H, Zhang J, Liu Z. Effect of hydrocarbons precursors on the formation of carbon nanotubes in chemical vapor deposition. Carbon 2004;42(4):829–35.
[32] Bartsch K, Arnold B, Kaltofen R, Täschner C, Thomas J, Leonhardt A. Effects of catalyst pre-treatment on the growth of single-walled carbon nanotubes by microwave CVD. Carbon 2007;45:543–52.
[33] Lohr SL. Sampling: design and analysis. Pacific Grove, CA: Duxbury Press; 1999.
[34] Park TJ, Banerjee S, Hemraj-Benny T, Wong SS. Purification strategies and purity visualization for single-walled carbon nanotubes. J Mater Chem 2006;16(2):141–54.
[35] Zhang M, Yudasaka M, Koshio A, Iijima S. Thermogravimetric analysis of single-wall carbon nanotubes ultrasonicated in monochlorobenzene. Chem Phys Lett 2002;364:420–6.
[36] Stanmore BR, Brilhac JF, Gilot P. The oxidation of soot: a review of experiments, mechanisms and models. Carbon 2001;39:2247–68.
[37] Arepalli S, Nikolaev P, Gorelik O, Hadjiev VG, Holmes W, Files B, et al. Protocol for the characterization of single-wall carbon nanotubes material quality. Carbon 2004;42:1783–91.
[38] Attal S, Thiruvengadathan R, Regev O. Determination of the concentration of single-walled carbon nanotubes in aqueous dispersions using UV–Visible absorption spectroscopy. Anal Chem 2006;78(23):8098–104.
[39] Landi BJ, Ruf HJ, Evans CM, Cress CD, Raffaelle RP. Purity assessment of single-wall carbon nanotubes, using optical absorption spectroscopy. J Phys Chem B 2005;109(20):9952–65.
[40] Landi BJ, Ruf HJ, Worman JJ, Raffaelle RP. Effects of alkyl amide solvents on the dispersion of single-wall carbon nanotubes. J Phys Chem B 2004;108(44):17089–95.
[41] Ryabenko AG, Dorofeeva TV, Zvereva GI. UV–VIS-NIR spectroscopy study of sensitivity of single-wall carbon nanotubes to chemical processing and Van-der-Waals SWCNT/SWCNT interaction. Verification of the SWCNT content measurements by absorption spectroscopy. Carbon 2004;42(8–9):1523–35.
[42] Itkis M, Perea DE, Jung R, Niyogi S, Haddon RC. Comparison of analytical techniques for purity evaluation of single-walled carbon nanotubes. J Am Chem Soc 2005;127(10):3439–48.
[43] Tan Y, Resasco DE. Dispersion of single-walled carbon nanotubes of narrow diameter distribution. J Phys Chem B 2005;109:14454–60.
[44] Itkis ME, Niyogi S, Meng M, Hamon M, Hu H, Haddon RC. Spectroscopic study of the Fermi level electronic structure of single-walled carbon nanotubes. Nano Lett 2002;2(2):155–9.